

Article

Characterization of Wear Properties of Pure Nickel Modified by Ni-Cr Composite and CaF₂ Solid Lubricant Addition

Mateusz Kotkowiak *  and Adam Piasecki * 

Institute of Materials Engineering, Faculty of Materials Engineering and Technical Physics, Poznan University of Technology, Jana Pawła II 24, 60-965 Poznan, Poland

* Correspondence: mateusz.kotkowiak@put.poznan.pl (M.K.); adam.piasecki@put.poznan.pl (A.P.)

Abstract: Nickel composites doped by chromium and calcium fluoride were produced by powder metallurgy. The friction coefficient of the samples containing 20% of the CaF₂ was lower at elevated temperatures (600 °C) than the friction coefficient for the Ni-50%NiCr(80/20) composite (0.14 vs. 0.20). Sample surfaces were analyzed by the scanning electron microscope (SEM). EDS analysis proved tribofilm formation on the surface of the sample with CaF₂ addition. A laser confocal microscope (LCM) was used to investigate the surface condition of the counter-sample after wear tests. The presence of the tribofilm reduced the wear of the frictional pair, and because of that the wear tracks were smooth. Tribofilm limited the abrasive wear and ploughing. Therefore, the tribofilm protected the sample and counter-sample from wear.

Keywords: calcium fluoride; self-lubricating material; surface analysis; confocal microscopy



Citation: Kotkowiak, M.; Piasecki, A. Characterization of Wear Properties of Pure Nickel Modified by Ni-Cr Composite and CaF₂ Solid Lubricant Addition. *Materials* **2022**, *15*, 7511. <https://doi.org/10.3390/ma15217511>

Academic Editor: Christian Müller

Received: 21 September 2022

Accepted: 20 October 2022

Published: 26 October 2022

Publisher's Note: MDPI stays neutral with regard to jurisdictional claims in published maps and institutional affiliations.



Copyright: © 2022 by the authors. Licensee MDPI, Basel, Switzerland. This article is an open access article distributed under the terms and conditions of the Creative Commons Attribution (CC BY) license (<https://creativecommons.org/licenses/by/4.0/>).

1. Introduction

Nowadays, nickel-based materials are very common because of their interesting properties such as high corrosion resistance. On the other hand, the main disadvantages of these materials are poor wear resistance and low hardness. Despite that fact, nickel-based materials have been widely used in different applications such as the automotive, shipbuilding, and aviation industries, as well as in nuclear reactors, which means they are exposed to high temperatures; hot corrosion; an aggressive environment; and wear at different, even very high, temperatures. Because of these difficult conditions, Ni-based materials have to be modified. Conventional Ni-based alloys could be modified by powder boriding [1,2], fluidized bed technology [3], paste boronization [4], or laser alloying [5,6]. Currently, ceramics materials based on nickel are very common, although they can be doped by other elements or chemical compounds. Nickel is often modified with additions of chromium, molybdenum, cobalt, or copper. Chromium is used to increase corrosion resistance at normal and elevated temperatures, as well as heat resistance. The addition of molybdenum increases the resistance to reducing acid. If copper is added to nickel, alloys will be characterized by high corrosion resistance in alkaline solutions, salts, and seawater. Moreover, Cobalt increases corrosion resistance at high temperatures [7,8]. One of the most frequently used nickel-based ceramics composites are Ni-Cr composite materials with varying additions of chromium or its compounds [9–12]. Additionally, because of their good properties, the Ni-Cr composites have been widely used as a coating material, to modify other materials, for example, stainless steel [13–16]. As Ni-Cr ceramic composites are so widely used, it is important to improve their wear properties, especially at high temperature. A possible way to strengthen the tribological properties of these materials is to modify them by adding solid lubricants. Solid lubricants have been divided into three groups, which differ in application temperature: –200 °C to room temperature (RT), and RT to 500 °C and above 500 °C [17,18]. Soft metals (Ag) [19–21], sulfides (MoS₂, WS₂) [22–26], and polymers (PTFE) [27] belong to moderate solid lubricant. Fluorides (BaF₂,

CaF₂) [28–31], oxides (ZnO, PbO, and TiO₂) [32,33], and salts (BaSO₄, CaSO₄) [34] form the group of high-temperature solid lubricants. The connection of Ni-based composite and self-lubricant, called self-lubricating materials, could be obtained by many methods: cold pressing and sintering [35], hot pressing and sintering [36], and spark-plasma sintering [37].

In this work, the Ni-based composites with the addition of NiCr(80/20) and CaF₂ were investigated. Samples were produced by powder metallurgy. The first step was pressing by the hydraulic press followed by sintering carried out at 1000 °C for 2 h. Wear tests were conducted at room and at elevated temperatures, after tests samples were investigated by SEM and confocal microscopy.

2. Experimental Methods

2.1. Powder Metallurgy

The first step of the investigation was powder preparation. Powder particles are shown in the Supplementary Materials (Figure S1). Ni and Ni–Cr(80/20) powders are characterized by a spheroidal shape, whereas the particles of CaF₂ have a cuboidal shape. The size of the particles did not exceed 10 µm (Figure S1a). Two powder mixtures were prepared: the first mixture contained 50 wt.% of pure Ni and 50 wt.% of NiCr(80/20), while the second mixture contained 40 wt.% of pure Ni, 40 wt.% of NiCr(80/20) and 20 wt.% of CaF₂. The next step was pressing and sintering. Powder mixtures were pressed by the MP250M hydraulic press. The pressing pressure was equal to 11,952 kgf/cm² (1.17 GPa). Sintering was conducted at 1200 °C in an inert atmosphere to avoid the oxidation of the samples. The heating rate was 250 °C/h, and so was the cooling rate [38].

2.2. Wear Tests

The pin-on-disc method was used to investigate the tribological properties of the composites. A detailed description of this method is described in the previous paper [32]. The parameters of the experiment were as follows: temperature (from room temperature (RT) to 600 °C), time (1 h), the rotational speed of the counter-sample (120 min^{−1}), and the load (4.9 N). The scheme and tribotester are shown in Figure 1.

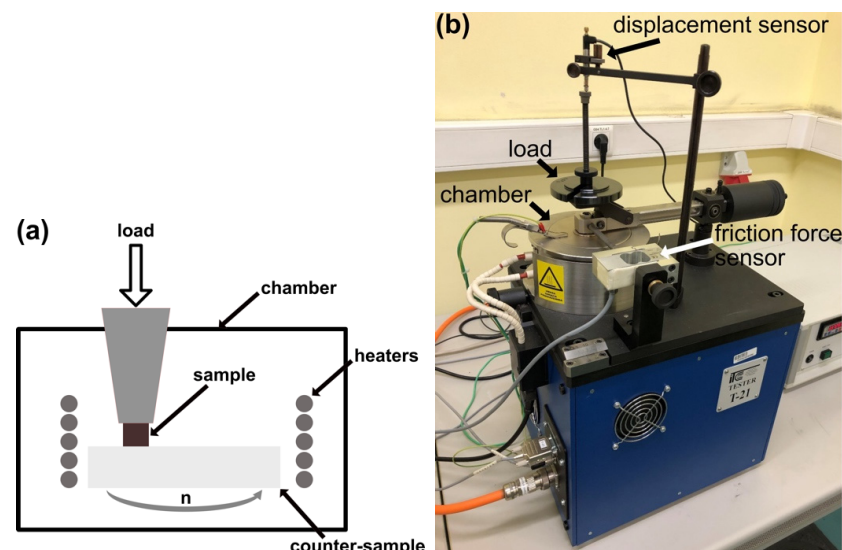


Figure 1. Pin-on-disc experiment: (a) scheme of the chamber, (b) T21 tribotester.

2.3. Surface Analysis

Scanning electron microscope (SEM)—Tescan MIRA3 Brno, The Czech Republic—and optical microscope (OM)—Opta-Tech 40LAB, Warsaw, Poland—were used to investigate the surface conditions of the worn samples.

SEM investigations was conducted in contrast to the secondary electron (SE) and backscattered electrons (BSE). The BSE contrast is beneficial because it gives information

about chemical composition diversity. The areas that contain light elements are dark, whereas heavy elements are bright. Additionally, sample surfaces were analyzed by the EDS method. The microanalyzer (Ultim[®] Max 65, Oxford Instruments, High Wycombe, UK) was used to detect the elements appearing on the surface of the sample. Calcium, fluorine, nickel, chromium, and oxygen were analyzed. The results of the EDS analysis were shown in one color-element concentration map and in twelve color-scale maps. In this investigation, the accelerating voltage equal to 12 kV was used because the interaction volume has to be limited.

2.4. Confocal Microscopy

The confocal microscope (LSM 710, Carl Zeiss, Oberkochen, Germany), equipped with an HeNe laser with a wavelength of 543 nm, was used to investigate the surface of the samples after the wear test. Additionally, changes of roughness and the stereometrics profiles of samples were analyzed.

3. Results and Discussion

Composites were characterized by low porosity; additionally, the particles of CaF₂ were evenly distributed in the matrix, which means the parameters of sample preparation were appropriate (Figure S2 in Supplement materials). Therefore, the wear test could be carried out.

Figure 2 shows the variation of friction coefficient (μ) for samples with and without the addition of the CaF₂ at room temperature. The first stage of wear—grinding-in—lasted approximately 520 s for the Ni–50% NiCr composite and 1020 s for the sample with CaF₂ addition. During the test conducted at RT, the average friction coefficient (μ_a) for Ni–NiCr was lower than that for the self-lubricating composite (0.77 vs. 0.83). Figure 2 shows the surface of the counter-sample after the wear test. The surfaces were different: shallow grooves could be observed on the surface of the counter-specimen combined with composite without solid lubricant addition (Figure 3a). However, in Figure 3b, signs of previous machining were visible.

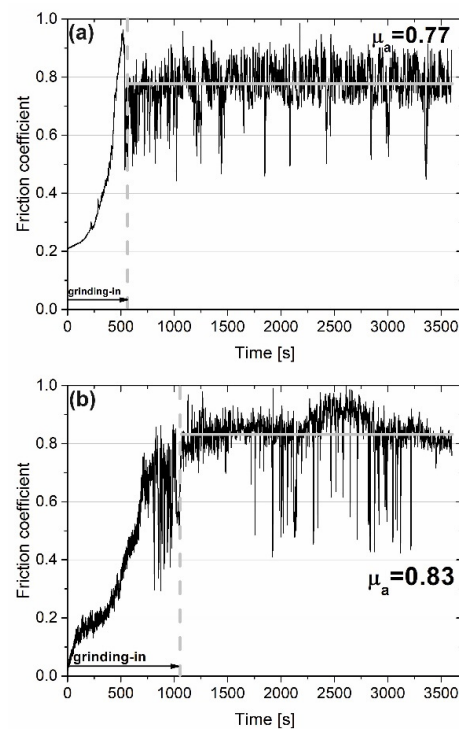


Figure 2. Results of wear test conducted at room temperature for sintered Ni-50%NiCr(80/20) (a) and Ni-40%NiCr(80/20)-20%CaF₂ (b) (friction coefficient vs. time of friction).

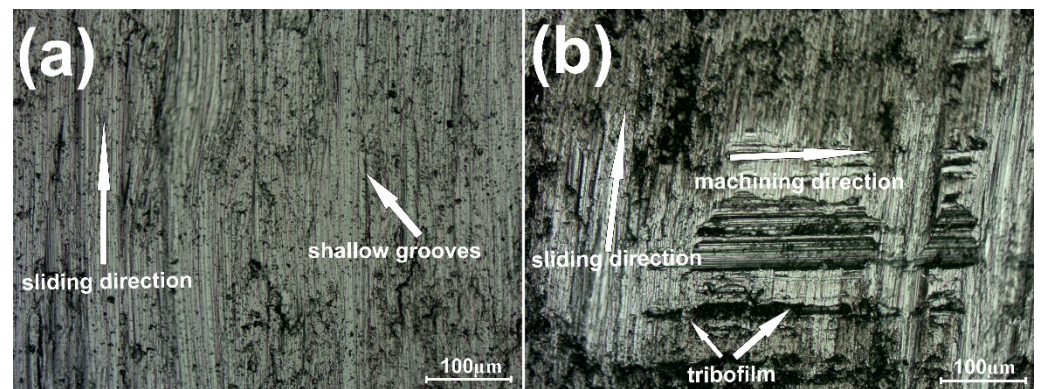


Figure 3. Surface condition of the counter-specimen mating with Ni-50%NiCr(80/20) (a) and Ni-40%NiCr(80/20)-20%CaF₂ (b), after wear test conducted at room temperature.

When the temperature of wear investigation increased to 200 °C, the course of the friction coefficient changed significantly (Figure 4). Grinding-in times were as follows: for the self-lubricating composite, approximately 1300 s; and for the composite without CaF₂ addition, approximately 300 s. The μ_a value for the Ni–NiCr composite was 0.63, but after 2250 s it increased to 0.86. It may have been caused by adhesive wear, which meant that wear products were located between the mating parts. The μ_a for the sample with the addition of CaF₂ was higher and equal to 0.69. Figure 5 shows the surface of the counter-specimens mated with samples. The signs of intensive abrasive wear were observed on the counter-specimen combined with the Ni–NiCr composite (Figure 5a). On the surface of the second counter-specimen, tribofilm was observed and, as a result, machining scratches were still visible after the wear test (Figure 5b).

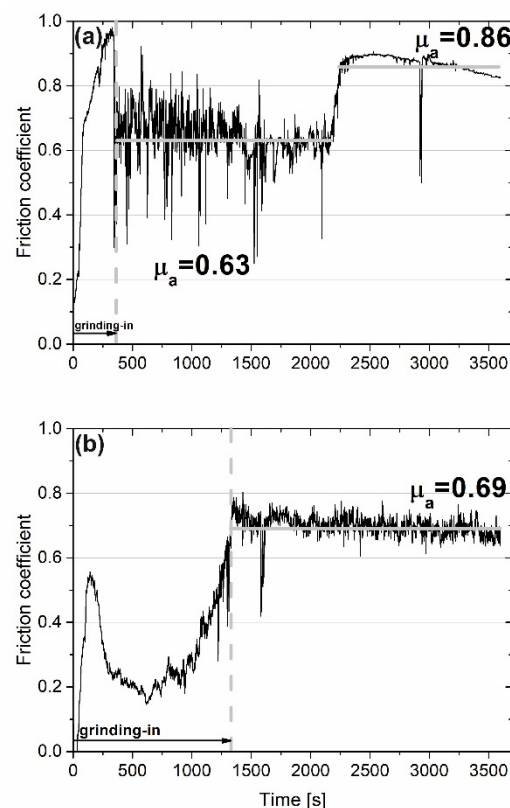


Figure 4. Results of wear test conducted at 200 °C for sintered Ni-50%NiCr(80/20) (a) and Ni-40%NiCr(80/20)-20%CaF₂ (b) (friction coefficient vs. time of friction).

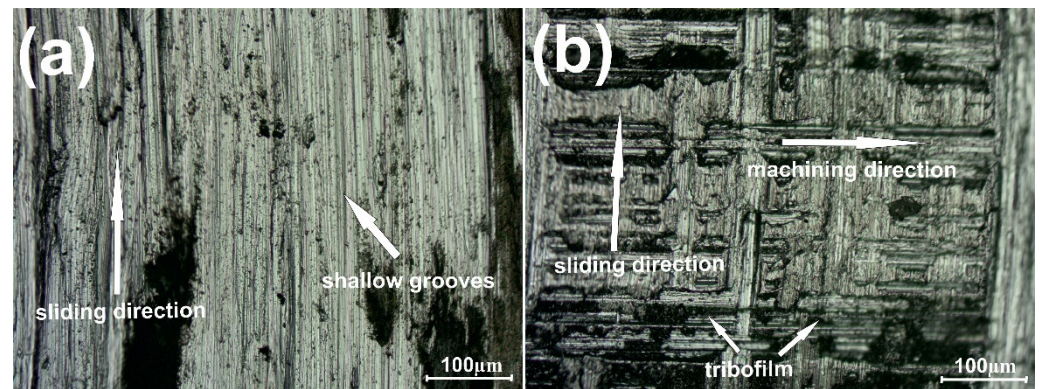


Figure 5. Surface condition of the counter-specimen mating with Ni-50%NiCr(80/20) (a) and Ni-40%NiCr(80/20)-20%CaF₂ (b), after wear test conducted at 200 °C.

Figure 6 shows the variation of the friction coefficient during the wear test conducted at 400 °C. The grinding-in stage lasted approximately 300 s for the Ni–NiCr composite. After this time, the μ_a value was equal to 0.79 because of adhesive wear. However, after 1600 s, the average value of friction coefficient dropped drastically to 0.51. In the case of the self-lubricating composite, the first stage of wear—grinding-in—lasted approximately 700 s. After the grinding-in, the friction coefficient was stable over time and the μ_a was equal to 0.55. Differences between surfaces of counter-specimens mated with the Ni–NiCr composite and the self-lubricating composite are shown in Figure 7. Shallow grooves can be seen in Figure 7a, whereas tribofilm and previous machining signs are visible in Figure 7b.

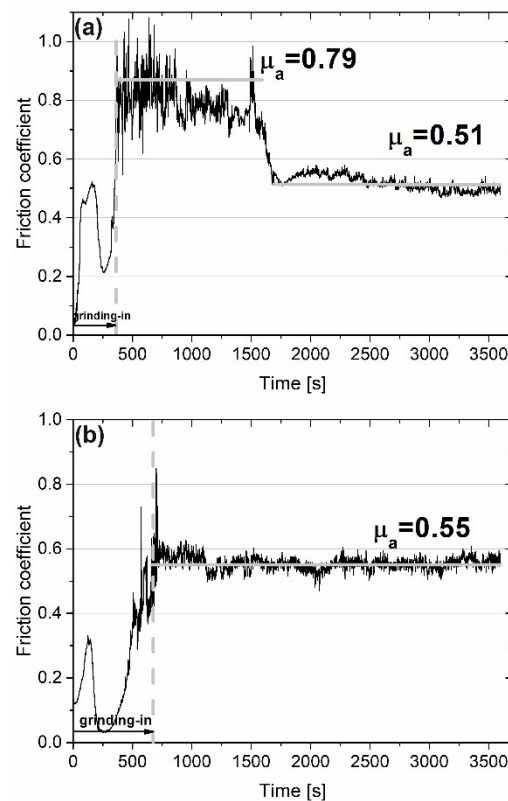


Figure 6. Results of wear test conducted at 400 °C for sintered Ni-50%NiCr(80/20) (a) and Ni-40%NiCr(80/20)-20%CaF₂ (b) (friction coefficient vs. time of friction).

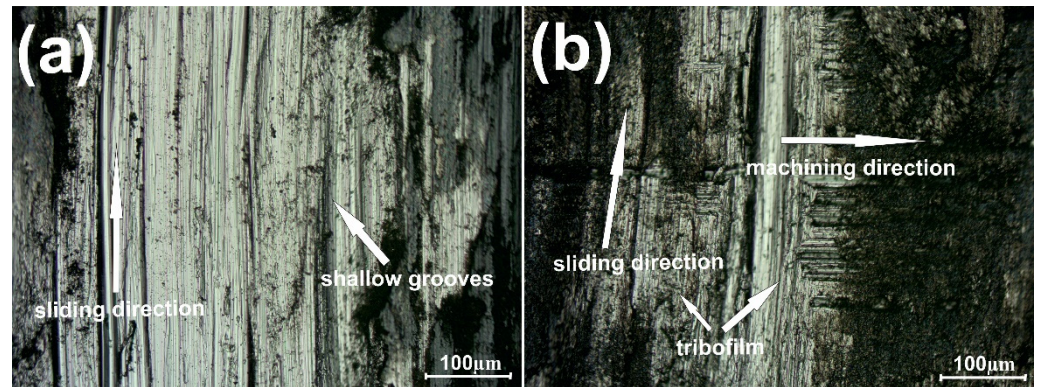


Figure 7. Surface condition of the counter-specimen mating with Ni-50%NiCr(80/20) (a) and Ni-40%NiCr(80/20)-20%CaF₂ (b), after wear test conducted at 400 °C.

The results of wear investigation conducted at 600 °C are shown in Figure 8. At this temperature, the situation was different in comparison with RT, 200 °C and 400 °C. The grinding-in stage lasted longer for the sample without the addition of CaF₂ (1350 s vs. 750 s). Additionally, the average friction coefficient (μ_a) was lower for the sample with CaF₂ addition (0.14 vs. 0.20). It formed because CaF₂ is a high-temperature solid lubricant, and it has good lubrication properties above 500 °C. On the surface of the counter-sample combined with the Ni–NiCr composite, signs of intensive abrasive wear, i.e., shallow grooves, were visible (Figure 9a). However, on the counter-sample mated with self-lubricating, the composite traces of previous machining could be observed as well as tribofilm, which was produced during wear (Figure 9b).

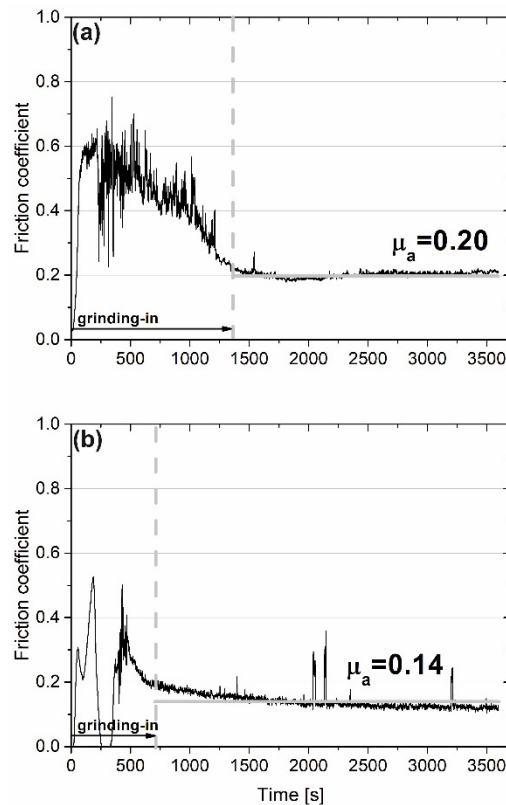


Figure 8. Results of wear test conducted at 600 °C for sintered Ni-50%NiCr(80/20) (a) and Ni-40%NiCr(80/20)-20%CaF₂ (b) (friction coefficient vs. time of friction).

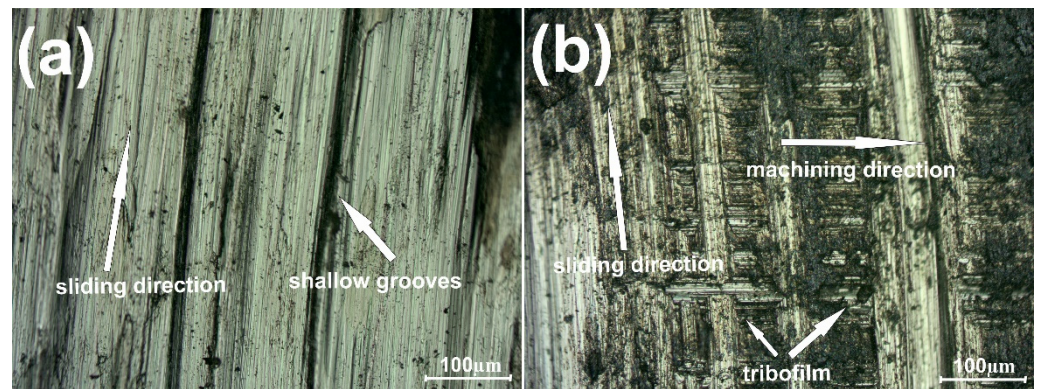


Figure 9. Surface condition of the counter-specimen mating with Ni-50%NiCr(80/20) (a) and Ni-40%NiCr(80/20)-20%CaF₂ (b), after wear test conducted at 600 °C.

Higher values of average friction coefficient and grinding-in times at room temperature, 200 °C, and 400 °C may have been caused by the relatively low temperature of the test. CaF₂ is well known as a high-temperature solid-lubricant, which obtains the best lubrication properties above 500 °C. Below that temperature, CaF₂ is too stiff, and it could not be smeared along the slip planes.

In Figures 10–13, stereometrics profiles of counter-specimen surfaces and graphs with detailed changes in the height of counter-samples after wear test are shown. A comparison between the Ni–NiCr composite and the self-lubricating composite, tested at RT, is visible in Figure 10. It can be clearly seen that surface of the Ni–NiCr composites was rough, and the level of difference between the material and wear track (ΔZ) was greater than ΔZ for the self-lubricating composite (5.42 vs. 2.1).

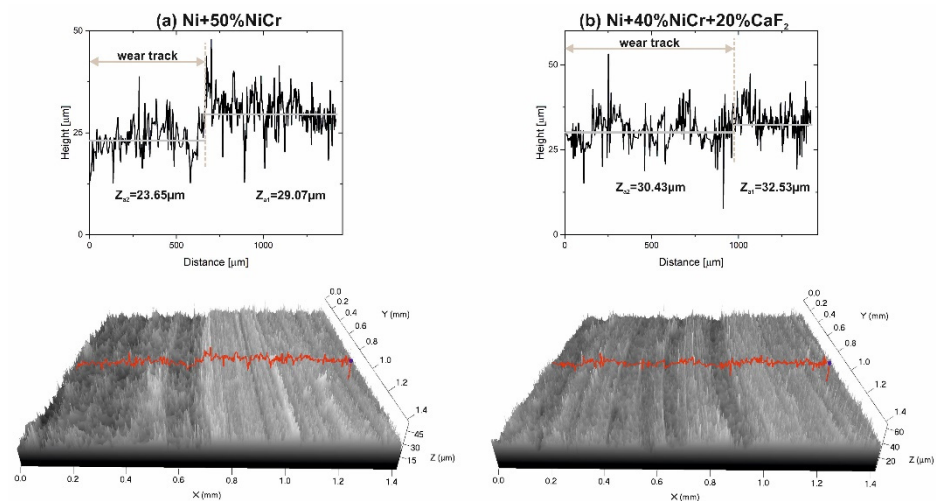


Figure 10. Stereometrics profiles of the counter-samples combined with Ni-50%NiCr(80/20) (a) and Ni-40%NiCr(80/20)-20%CaF₂ (b), after wear test at room temperature.

After the wear test conducted at 200 °C, the surface condition of the counter-sample mated with the Ni–NiCr composite was different (Figure 11a). The surface was smooth, but ΔZ value was very high, equal to 6.88. This may have been caused by adhesive wear, which meant that some parts of counter-sample were removed and stuck to sample surface. In the case of the counter-sample combined with the self-lubricating composite (Figure 11b), the profiles of the wear track and the base materials were similar and ΔZ was equal to 2.28.

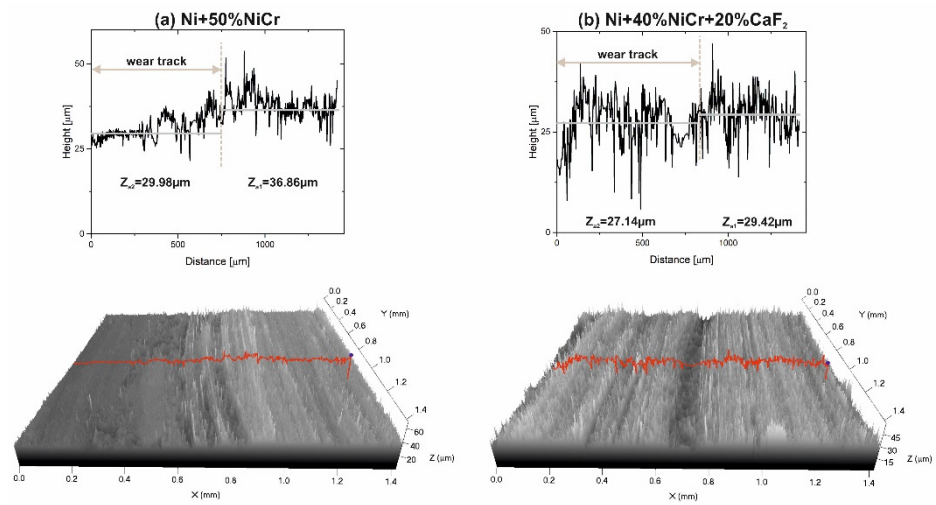


Figure 11. Stereometrics profiles of the counter-samples combined with Ni-50%NiCr(80/20) (a) and Ni-40%NiCr(80/20)-20%CaF₂ (b), after wear test at 200 °C.

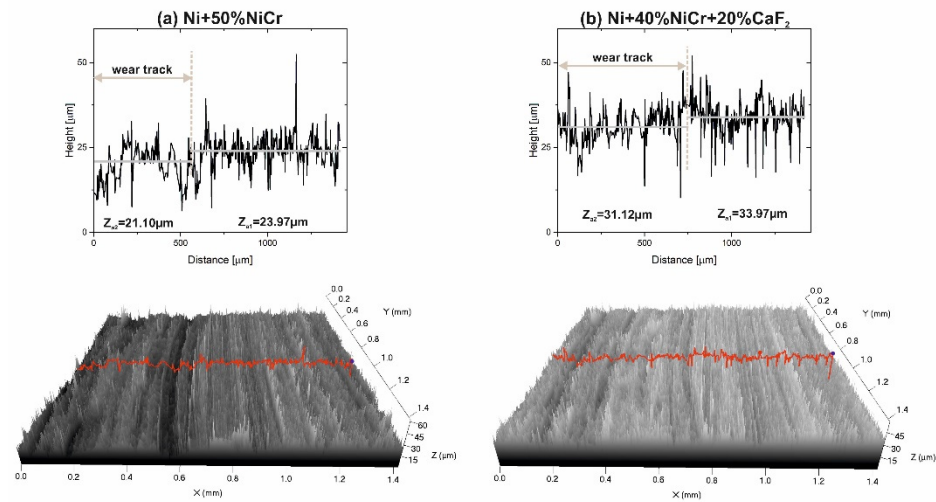


Figure 12. Stereometrics profiles of the counter-samples combined with Ni-50%NiCr(80/20) (a) and Ni-40%NiCr(80/20)-20%CaF₂ (b), after wear test at 400 °C.

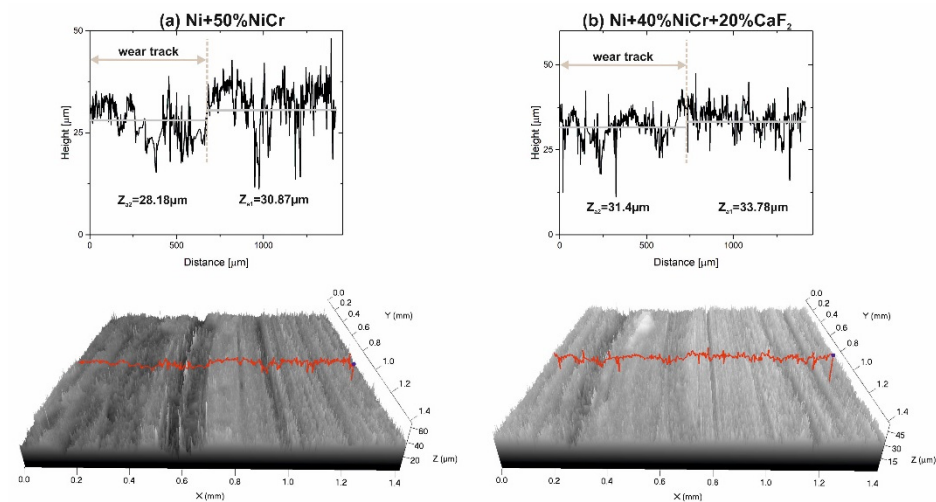


Figure 13. Stereometrics profiles of the counter-samples combined with Ni-50%NiCr(80/20) (a) and Ni-40%NiCr(80/20)-20%CaF₂ (b), after wear test at 600 °C.

In Figure 12, the results of the investigation of the surfaces of the counter-samples tested at 400 °C are shown. On the stereometrics profile of the counter-sample mated with the Ni–NiCr composites, scratches were visible and the ΔZ value was equal to 2.87. If the counter-specimen was combined with self-lubricating composites, its surface looked different because only shallow grooves were observed (the ΔZ value was slightly lower (2.85 vs. 2.87)).

In Figure 13a, the surface condition of the counter-sample used with Ni–NiCr composite at 600 °C is shown. In this figure, numerous deep scratches were observed. The surface condition of the counter-samples mated with self-lubricating composites at 600 °C are visible in Figure 13b. The shallow grooves, as well as signs of adhesive wear, were observed on the surface of the counter-sample. ΔZ value for counter-sample combined with composite without CaF_2 and with CaF_2 were comparable and equal to 2.69 and 2.38, respectively.

A confocal microscopy investigation exhibited beneficial properties of tribofilm because it protected the sample and counter-sample against wear. The main wear mechanism for Ni–NiCr composites was abrasive wear, which was revealed by deep scratches; also, level differences (ΔZ) between base material and wear track were higher (Figure 14). In the case of self-lubricating composites, some shallow grooves were observed on the surface.

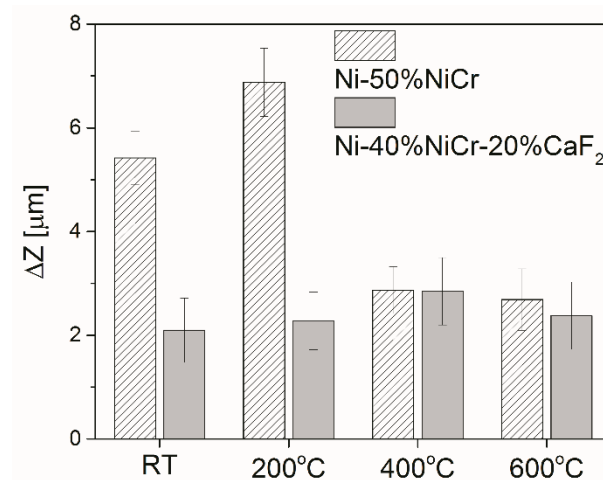


Figure 14. Level differences between the base material and wear track (ΔZ) of the counter-specimens.

The surface conditions of samples and counter-samples after wear tests showed a great deal of information about the friction process and the wear mechanism. The surface conditions of the samples after the wear test conducted at different temperatures are shown in Figure 15. Shallow grooves were visible on the surface of Ni–NiCr composites, which appeared at all investigated temperatures. Additionally, at room temperature, delamination occurred. The surfaces of the self-lubricating composites were different. Tribofilm consisting of CaF_2 was observed on sample surfaces, and tribofilm was characterized by varying thicknesses. The results of the EDS analysis are shown in Figures 16 and 17. The following elements were investigated: Ni and Cr (the main elements of the samples), Ca and F (the main elements of solid lubricant), and O (to identify if oxidative wear occurred). In the case of Ni–NiCr (Figure 16) composite, the EDS analysis confirmed the presence of nickel and chromium. Additionally, increased oxygen content was observed on sample surfaces tested at 200 °C, 400 °C, and 600 °C. On the surfaces of the self-lubricating composites, an increased amount of Ca, F, Ni, and Cr was observed (Figure 17). Moreover, increased content of Ca and F occurred in places where the amount of Ni and Cr was reduced, because samples were covered by tribofilm. Increased content of O was observed on samples' surfaces after a wear test conducted at elevated temperatures (200 °C, 400 °C, and 600 °C). Moreover, tribofilm protected samples against oxidation because the oxygen content was low in places where tribofilm formed.

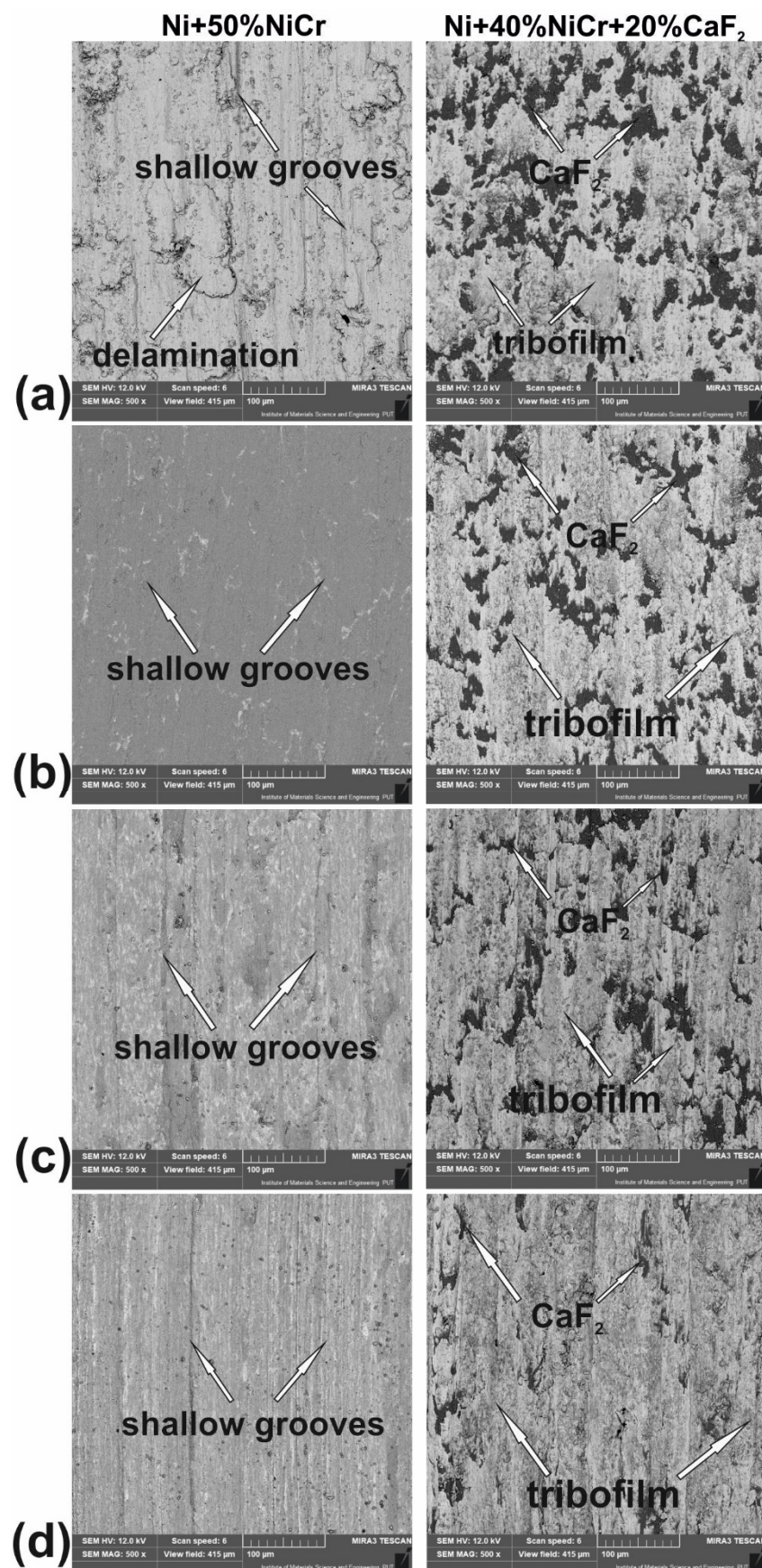


Figure 15. Surface condition of the sintered Ni-50%NiCr(80/20) and Ni-40%NiCr(80/20)-20%CaF₂ after wear test at room temperature, (a) at 200 °C, (b) at 400 °C, (c) at 600 °C, and (d) (SEM).

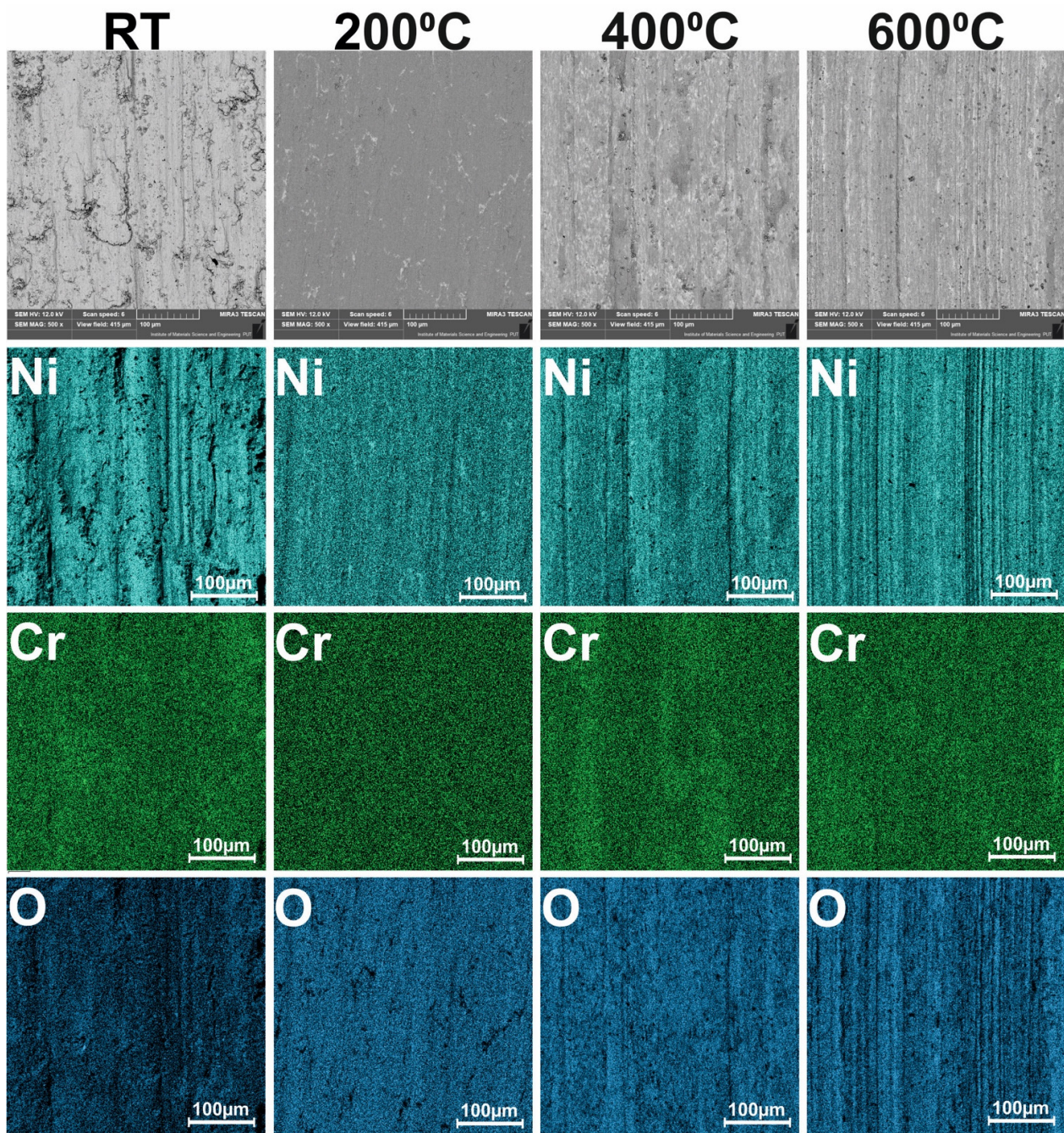


Figure 16. Results of EDS analysis of the worn Ni-50%NiCr(80/20) samples tested at different temperatures.

Figure 18 shows differences in the distribution of Ca on the surfaces of samples in 12-color scale. White areas contained a large amount of Ca, whereas in black areas, Ca was not detected. Thus, it was proved that tribofilm was characterized by diversified thickness. At room temperature and at 200 °C, there were more zones with brighter colors than at 400 °C and 600 °C. Differences emerged because CaF_2 was not smeared very well on the surfaces of samples; therefore, numerous CaF_2 clusters were observed. The situation changed at higher temperatures (400 °C and 600 °C). Then, CaF_2 particles reached higher temperature and smeared very well on the surface of the sample. On the sample tested at 600 °C, numerous areas with similar intensity were observed, which meant that the tribofilm thickness was comparable.

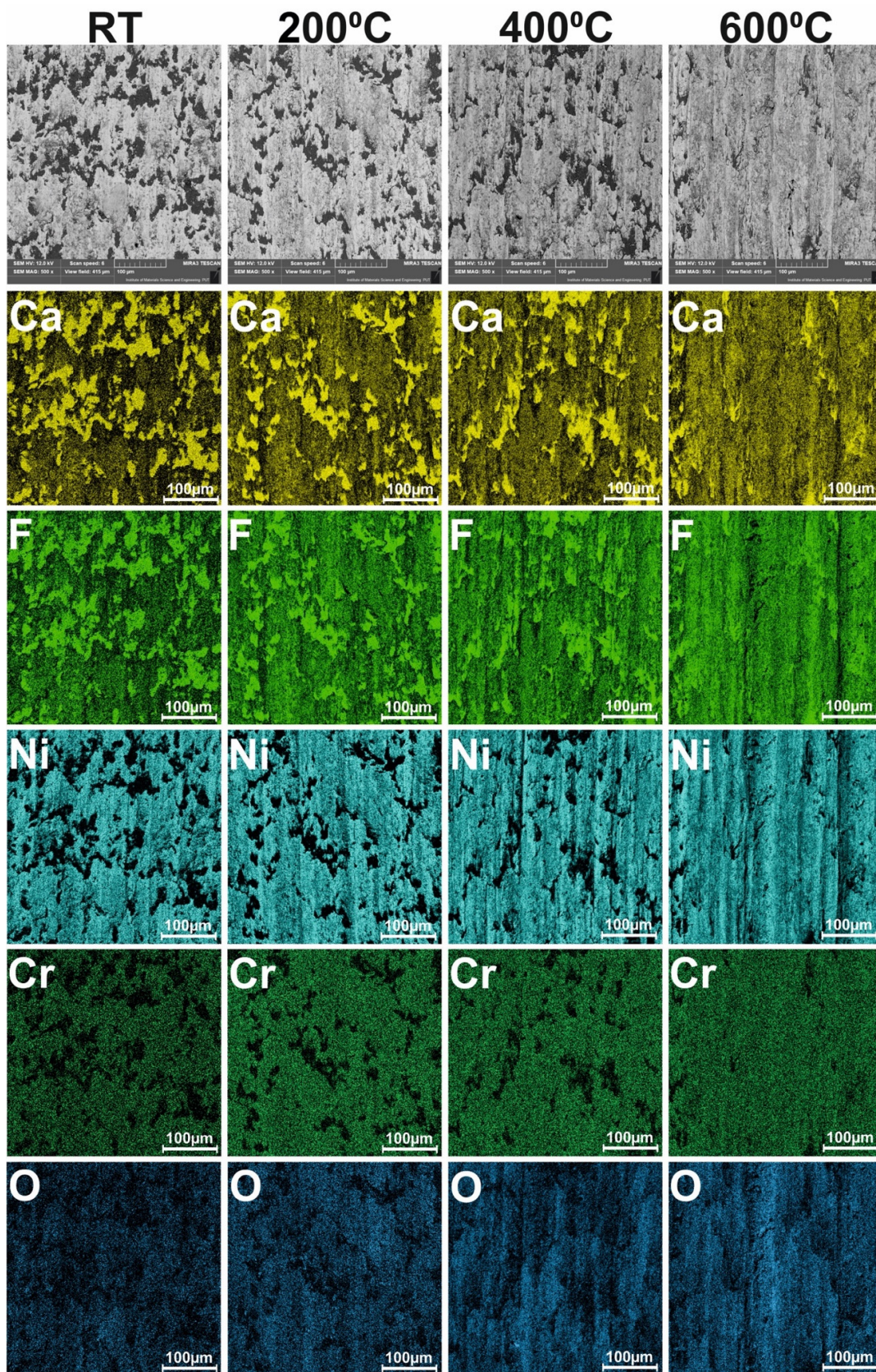


Figure 17. Results of EDS analysis of the worn Ni-40%NiCr(80/20)-20%CaF₂ samples tested at different temperatures.

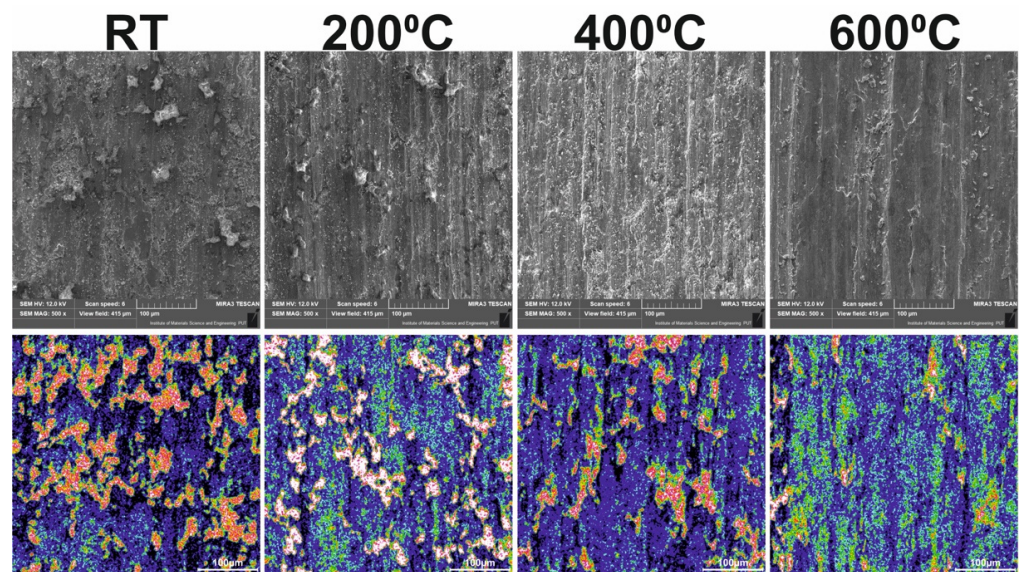


Figure 18. SEM and EDS images of the calcium concentration on the surface of the samples tested at different temperatures.

It could be clearly seen that tribofilm protected samples against wear, thus producing lower values of the average friction coefficient (Table 1, Figure 19). The composites with the addition of CaF_2 were characterized by lower values of μ_a at 200 °C and 600 °C, but on the other hand, at RT and 400 °C the μ_a were higher. When the values of μ_a were compared to the Figure 18, it could be clearly seen that on the surface of the composites tested at RT and 400 °C there were a lot of areas where CaF_2 was not detected (black color), and this probably caused the higher values of μ_a .

Table 1. Average friction coefficient (μ_a) of investigated materials.

	RT	200 °C	400 °C	600 °C
	μ_a			
Ni + 50 wt.% NiCr	0.77 ± 0.01	0.86 ± 0.01	0.51 ± 0.01	0.20 ± 0.01
Ni + 40 wt.% NiCr + 20 wt.% CaF_2	0.83 ± 0.01	0.69 ± 0.01	0.55 ± 0.01	0.14 ± 0.01

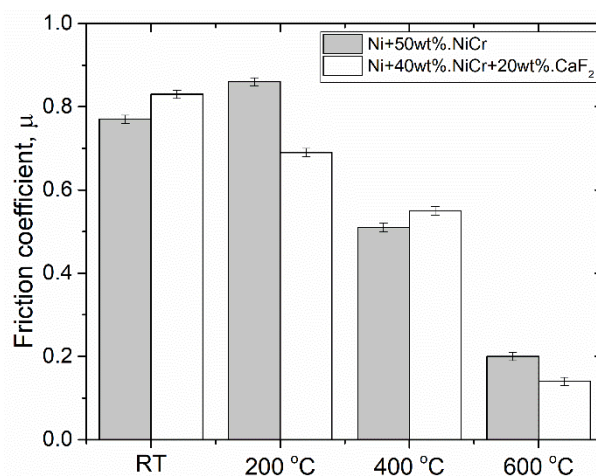


Figure 19. Average friction coefficient (μ_a) of investigated materials.

At 600 °C, the average friction coefficient was equal to 0.14 for the Ni-Cr composite with the addition of CaF_2 . The highest values of the coefficient of friction at 600 °C

were observed for the Ni–Cr–Mo–Al composite with the addition of Ag and BaF₂/CaF₂ (approximately 0.3 in air and 0.16 in vacuum) [39]. Similar results of the friction coefficient were obtained in work [40]. Self-lubricating NiCr(80/20) composites with the addition of the following solid lubricants: Cr₂O₃ (20 wt.%), Ag (10 wt.%), and the eutectic mixture—BaF₂/CaF₂ (10 wt.%), were produced in work [41]. The lowest friction coefficients were at RT (~0.37), 200 °C (~0.33), and 400 °C (~0.32), which was probably caused by the addition of Ag, which is a moderate-temperature solid lubricant [17]. At 600 °C, the friction coefficient was equal to ~0.33, and it was two times higher than μ_a in this work. Additionally, the Ni alloy could be modified by the addition of 5% wt. CaF₂ and 20 wt.% MoS₂, and the friction coefficient, decreased from 0.41 at RT to 0.16 at 700 °C [42].

4. Conclusions

In this paper wear, the properties of the Ni–50%NiCr composite with and without the addition of CaF₂ were investigated. The microstructure of the self-lubricating composites was beneficial because CaF₂ particles were evenly distributed in the Ni–NiCr matrix.

1. At room temperature, the friction coefficient of the self-lubricating composite was higher than that of the composite without the addition of solid lubricant.
2. At 200 °C, initially, the μ_a value for the Ni–NiCr composite was lower than the value for the self-lubricating composite (0.63 vs. 0.69), but after some time, adhesive wear became the main wear mechanism and μ_a increased to 0.86.
3. At 400 °C, the μ_a value for the composite without the addition of CaF₂ was equal to 0.79, and after 1500 s this value dropped to 0.51, whereas the average friction coefficient for the self-lubricating composite was equal to 0.55.
4. At 600 °C, the average friction coefficient was lower for the self-lubricating composite in relation to the Ni–NiCr composite (0.14 vs. 0.20).
5. Grinding-in times were lower for the sample without the addition of solid-lubricant at room temperature, 200 °C, and 400 °C. However, at 600 °C, the grinding-in time for the self-lubricating composite was approximately two times lower than for the Ni–NiCr composite (720 s vs. 1350 s).
6. A surface analysis of the samples proved that the self-lubricating composite was coated by the thin tribofilm layer. EDS analysis showed that tribofilm consisted of calcium and fluorine and was characterized by diversified thickness.
7. The EDS analysis confirmed that tribofilm was well smeared on the sample surface at higher temperatures (400 °C and 600 °C) and the tribofilm protected samples against oxidation.

Supplementary Materials: The following supporting information can be downloaded at: <https://www.mdpi.com/article/10.3390/ma15217511/s1>, Figure S1: The powders used in this investigation: pure Ni (a), Ni–Cr (80/20) (b) and CaF₂ (c). Figure S2: Microstructure of produced sinters: Ni + Ni–Cr (a) and Ni + Ni–Cr + 20%CaF₂ (b).

Author Contributions: Conceptualization, M.K.; formal analysis, M.K., A.P.; funding acquisition, M.K.; investigation, M.K., A.P.; methodology, M.K., A.P.; project administration, M.K.; resources, M.K., A.P.; supervision, M.K.; validation, M.K., A.P.; visualization, M.K., A.P.; writing—original draft, M.K.; and writing—review and editing, M.K., A.P. All authors have read and agreed to the published version of the manuscript.

Funding: This work has been financially supported by National Science Centre as a part of the 2016/21/N/ST8/03555 project and in part by the Polish Ministry of Science and Higher Education.

Institutional Review Board Statement: Not applicable.

Informed Consent Statement: Not applicable.

Data Availability Statement: The data presented in this study are available on request from the corresponding author.

Conflicts of Interest: The authors declare no conflict of interest.

References

1. Özbek, I.; Akbulut, H.; Zeytin, S.; Bindal, C.; Ucisik, A.H. The Characterization of Borided 99.5% Purity Nickel. *Surf. Coat. Technol.* **2000**, *126*, 166–170. [\[CrossRef\]](#)
2. Mu, D.; Shen, B.-I.; Yang, C.; Zhao, X. Microstructure Analysis of Boronized Pure Nickel Using Boronizing Powders with SiC as Diluent. *Vacuum* **2009**, *83*, 1481–1484. [\[CrossRef\]](#)
3. Anthymidis, K.G.; Zinoviadis, P.; Roussos, D.; Tspas, D.N. Boriding of Nickel in a Fluidized Bed Reactor. *Mater. Res. Bull.* **2002**, *37*, 515–522. [\[CrossRef\]](#)
4. Lou, D.C.; Solberg, J.K.; Akselsen, O.M.; Dahl, N. Microstructure and Property Investigation of Paste Boronized Pure Nickel and Nimonic 90 Superalloy. *Mater. Chem. Phys.* **2009**, *115*, 239–244. [\[CrossRef\]](#)
5. Piasecki, A.; Kotkowiak, M.; Makuch, N.; Kulka, M. Wear Behavior of Self-Lubricating Boride Layers Produced on Inconel 600-Alloy by Laser Alloying. *Wear* **2019**, *426–427*, 919–933. [\[CrossRef\]](#)
6. Kulka, M.; Dziarski, P.; Makuch, N.; Piasecki, A.; Miklaszewski, A. Applied Surface Science Microstructure and Properties of Laser-Borided Inconel 600-Alloy. *Appl. Surf. Sci.* **2013**, *284*, 757–771. [\[CrossRef\]](#)
7. Knosalla, C.; Lau, M.; Schmies, L.; Lippmann, W.; Hurtado, A. Investigation on the Corrosion Behavior of Nickel-Base Alloys in Molten Chlorides for Sensible Heat Energy Applications. *Adv. Eng. Mater.* **2020**, *22*, 2000099. [\[CrossRef\]](#)
8. Kotkowiak, M.; Piasecki, A.; Kotkowiak, M.; Kulka, M. Heat-Resisting Aluminized Coatings Modified by Chromium Addition Produced on Nickel-Based Alloys. *Trans. Indian Inst. Met.* **2018**, *71*, 2919–2931. [\[CrossRef\]](#)
9. Ouyang, J.H.; Shi, C.C.; Liu, Z.G.; Wang, Y.M.; Wang, Y.J. Fabrication and High-Temperature Tribological Properties of Self-Lubricating NiCr-BaMoO₄ Composites. *Wear* **2015**, *330–331*, 272–279. [\[CrossRef\]](#)
10. Huang, X.-y.; Wang, J.h.; Zhang, H.q.; Ren, J.; Zan, Q.f.; Gong, Q.m.; Wu, B. WC-Ni-Cr-Based Self-Lubricating Composites Fabricated by Pulsed Electric Current Sintering with Addition of WS₂ Solid Lubricant. *Int. J. Refract. Met. Hard Mater.* **2017**, *66*, 158–162. [\[CrossRef\]](#)
11. Li, Y.F.; Yin, H.; Li, X.L.; Mao, C.C. Friction and Wear Properties of Spark Plasma Sintering NiCr-SrSO₄ Composites at Elevated Temperatures in Sliding Against Alumina Ball. *Tribol. Lett.* **2016**, *64*, 29. [\[CrossRef\]](#)
12. Fattahi, Z.; Sajjadi, S.A.; Babakhani, A.; Saba, F. Ni–Cr Matrix Composites Reinforced with Nano- and Micron-Sized Surface-Modified Zirconia: Synthesis, Microstructure and Mechanical Properties. *J. Alloys Compd.* **2020**, *817*, 152755. [\[CrossRef\]](#)
13. Torgerson, T.B.; Mantri, S.A.; Banerjee, R.; Scharf, T.W. Room and Elevated Temperature Sliding Wear Behavior and Mechanisms of Additively Manufactured Novel Precipitation Strengthened Metallic Composites. *Wear* **2019**, *426–427*, 942–951. [\[CrossRef\]](#)
14. Harachai, K.; Kothanam, N.; Qin, J.; Boonyongmaneerat, Y.; Jaroenapibal, P. Hardness and Tribological Properties of Co-Electrodeposited Ni-W-B/B Coatings. *Surf. Coat. Technol.* **2020**, *402*, 126313. [\[CrossRef\]](#)
15. Zhao, Y.; Yu, T.; Chen, L.; Chen, Y.; Guan, C.; Sun, J. Microstructure and Wear Resistance Behavior of Ti–C–B₄C-Reinforced Composite Coating. *Ceram. Int.* **2020**, *46*, 25136–25148. [\[CrossRef\]](#)
16. Han, T.; Xiao, M.; Zhang, J.; Feng, X.; Shen, Y. Laser Cladding Composite Coating on Mild Steel Using Ni–Cr–Ti–B₄C Powder. *Surf. Eng.* **2020**, *36*, 1278–1284. [\[CrossRef\]](#)
17. Yang, J.F.; Jiang, Y.; Hardell, J.; Prakash, B.; Fang, Q.F. Influence of Service Temperature on Tribological Characteristics of Self-Lubricant Coatings: A Review. *Front. Mater. Sci.* **2013**, *7*, 28–39. [\[CrossRef\]](#)
18. Sarkar, M.; Mandal, N. Solid Lubricant Materials for High Temperature Application: A Review. *Mater. Today Proc.* **2022**, *66*, 3762–3768. [\[CrossRef\]](#)
19. Mohamad, W.F.; Khan, A.A.; Ahmad, F.; Yassin, A. Phase Analysis and Microstructure Study of Sintered Ni-Cr Composites Containing MoS₂, Ag and CaF₂ Additives as Solid Lubricants. *J. Mech. Eng. Sci.* **2020**, *14*, 6548–6556. [\[CrossRef\]](#)
20. Ding, C.H.; Liu, C.H.; Yang, Z.M.; Wang, Y.P.; Sun, Z.B.; Yu, L. Effect of Size Refinement and Distribution of Lubricants on Friction Coefficient of High Temperature Self-Lubricating Composites. *Compos. Sci. Technol.* **2010**, *70*, 1000–1005. [\[CrossRef\]](#)
21. Ye, F.; Lou, Z.; Wang, Y.; Liu, W. Wear Mechanism of Ag as Solid Lubricant for Wide Range Temperature Application in Micro-Beam Plasma Cladded Ni60 Coatings. *Tribol. Int.* **2022**, *167*, 107402. [\[CrossRef\]](#)
22. Xing, Y.; Deng, J.; Li, S.; Yue, H.; Meng, R.; Gao, P. Cutting Performance and Wear Characteristics of Al₂O₃/TiC Ceramic Cutting Tools with WS₂/Zr Soft-Coatings and Nano-Textures in Dry Cutting. *Wear* **2014**, *318*, 12–26. [\[CrossRef\]](#)
23. Rapoport, L.; Moshkovich, A.; Perflyev, V.; Lapsker, I.; Halperin, G.; Itovich, Y.; Etsion, I. Friction and Wear of MoS₂ Films on Laser Textured Steel Surfaces. *Surf. Coat. Technol.* **2008**, *202*, 3332–3340. [\[CrossRef\]](#)
24. Ren, S.; Shang, K.; Cui, M.; Wang, L.; Pu, J.; Yi, P. Structural Design of MoS₂-Based Coatings toward High Humidity and Wide Temperature. *J. Mater. Sci.* **2019**, *54*, 11889–11902. [\[CrossRef\]](#)
25. He, J.; Sun, J. Synergistic Lubrication Effect of Al₂O₃ and MoS₂ Nanoparticles Confined between Iron Surfaces: A Molecular Dynamics Study. *J. Mater. Sci.* **2021**, *56*, 9227–9241. [\[CrossRef\]](#)
26. Krauß, S.; Seynstahl, A.; Tremmel, S.; Meyer, B.; Bitzek, E.; Göken, M.; Yokosawa, T.; Zubiri, B.A.; Spiecker, E.; Merle, B. Structural Reorientation and Compaction of Porous MoS₂ Coatings during Wear Testing. *Wear* **2022**, *500–501*, 204339. [\[CrossRef\]](#)
27. Tan, B.; Stephens, L.S. Evaluation of Viscoelastic Characteristics of PTFE-Based Materials. *Tribol. Int.* **2019**, *140*, 105870. [\[CrossRef\]](#)
28. Jianxin, D.; Tongkun, C.; Zeliang, D.; Jianhua, L.; Junlong, S.; Jinlong, Z. Tribological Behaviors of Hot-Pressed Al₂O₃/TiC Ceramic Composites with the Additions of CaF₂ Solid Lubricants. *J. Eur. Ceram. Soc.* **2006**, *26*, 1317–1323. [\[CrossRef\]](#)
29. Deng, J.; Liu, L.; Yang, X.; Liu, J.; Sun, J.; Zhao, J. Self-Lubrication of Al₂O₃/TiC/CaF₂ Ceramic Composites in Sliding Wear Tests and in Machining Processes. *Mater. Des.* **2007**, *28*, 757–764. [\[CrossRef\]](#)

30. Murakami, T.; Ouyang, J.H.; Sasaki, S.; Umeda, K.; Yoneyama, Y. High-Temperature Tribological Properties of Al₂O₃, Ni-20 Mass% Cr and NiAl Spark-Plasma-Sintered Composites Containing BaF₂-CaF₂ Phase. *Wear* **2005**, *259*, 626–633. [[CrossRef](#)]
31. Ouyang, J.H.; Sasaki, S.; Umeda, K. The Friction and Wear Characteristics of Plasma-Sprayed ZrO₂-Cr₂O₃-CaF₂ from Room Temperature to 800 °C. *J. Mater. Sci.* **2001**, *36*, 547–555. [[CrossRef](#)]
32. Xu, Z.; Zhang, Q.; Zhai, W. Tribological Properties of TiAl Matrix Self-Lubricating Composites Incorporated with Tungsten Disulfide and Zinc Oxide. *RSC Adv.* **2015**, *5*, 45044–45052. [[CrossRef](#)]
33. Birleanu, C.; Pustan, M.; Cioaza, M.; Molea, A.; Popa, F.; Contiu, G. Effect of TiO₂ Nanoparticles on the Tribological Properties of Lubricating Oil: An Experimental Investigation. *Sci. Rep.* **2022**, *12*, 5201. [[CrossRef](#)] [[PubMed](#)]
34. Ouyang, J.H.; Li, Y.F.; Wang, Y.M.; Zhou, Y.; Murakami, T.; Sasaki, S. Microstructure and Tribological Properties of ZrO₂(Y₂O₃) Matrix Composites Doped with Different Solid Lubricants from Room Temperature to 800 °C. *Wear* **2009**, *267*, 1353–1360. [[CrossRef](#)]
35. Zhang, W.; Du, L.; Lan, H.; Huang, C.; Zhang, W. Wear Behavior of a NiCr/AgVO₃ Self-Lubricating Composite. *Acta Metall. Sin. (Engl. Lett.)* **2013**, *26*, 435–440. [[CrossRef](#)]
36. Zhang, P.; Zhao, G.; Wang, W.; Wang, B.; Shi, P.; Qi, G.; Yi, G. Study on the Mechanical and Tribological Properties and the Mechanisms of Cr-Free Ni-Based Self-Lubricating Composites at a Wide Temperature Range. *Metals* **2020**, *10*, 268. [[CrossRef](#)]
37. Ouyang, J.H.; Sasaki, S.; Murakami, T.; Umeda, K. Tribological Properties of Spark-Plasma-Sintered ZrO₂(Y₂O₃)-CaF₂-Ag Composites at Elevated Temperatures. *Wear* **2005**, *258*, 1444–1454. [[CrossRef](#)]
38. Kotkowiak, M.; Piasecki, A.; Kulka, M. The Influence of Solid Lubricant on Tribological Properties of Sintered Ni–20%CaF₂ Composite Material. *Ceram. Int.* **2019**, *45*, 17103–17113. [[CrossRef](#)]
39. Zhen, J.; Cheng, J.; Zhu, S.; Hao, J.; Qiao, Z.; Yang, J.; Liu, W. High-Temperature Tribological Behavior of a Nickel Alloy Matrix Solid-Lubricating Composite under Vacuum. *Tribol. Int.* **2017**, *110*, 52–56. [[CrossRef](#)]
40. Cheng, J.; Zhen, J.; Zhu, S.; Yang, J.; Ma, J.; Li, W.; Liu, W. Friction and Wear Behavior of Ni-Based Solid-Lubricating Composites at High Temperature in a Vacuum Environment. *Mater. Des.* **2017**, *122*, 405–413. [[CrossRef](#)]
41. Ding, C.H.; Li, P.L.; Ran, G.; Tian, Y.W.; Zhou, J.N. Tribological Property of Self-Lubricating PM304 Composite. *Wear* **2007**, *262*, 575–581. [[CrossRef](#)]
42. Zhen, J.; Cheng, J.; Li, M.; Zhu, S.; Long, Z.; Yang, B.; Yang, J. Lubricating Behavior of Adaptive Nickel Alloy Matrix Composites with Multiple Solid Lubricants from 25 °C to 700 °C. *Tribol. Int.* **2017**, *109*, 174–181. [[CrossRef](#)]